Available online at www.sciencedirect.com
ScienceDirect
Journal of Solid State Chemistry 181 (2008) 943–949
JOURNAL OF SOLID STATE CHEMISTRY
www.elsevier.com/locate/jssc

Syntheses, structures and magnetic properties of two new one-dimensional cobalt (II) phosphites with organic amines acting as ligands

Gaijuan Li, Yan Xing*, Shuyan Song

College of Chemistry, Northeast Normal University, 5268 Renmin Street, Changchun 130024, PR China

Received 5 August 2007; received in revised form 8 January 2008; accepted 14 January 2008
Available online 13 February 2008

Abstract

Two new one-dimensional (1D) inorganic–organic hybrid cobalt (II) phosphites $Co(HPO_3)$ (py) (**1**) and $[Co(OH)(py)_3][Co(py)_2][HPO_2(OH)]_3$ (**2**) have been prepared under solvothermal conditions in the presence of pyridine (py). Compound **1** crystallizes in the monoclinic system, space group $p2(1)/c$, $a = 5.3577(7)$ Å, $b = 7.7503(10)$ Å, $c = 17.816(2)$ Å, $\beta = 94.327(2)^\circ$, $V = 737.67(16)$ Å^3, $Z = 4$. Compound **2** is orthorhombic, $Cmcm$, $a = 16.3252(18)$ Å, $b = 15.7005(16)$ Å, $c = 13.0440(13)$ Å, $\beta = 90.00^\circ$ $V = 3343.4(6)$ Å^3 and $Z = 4$. Compound **1** possesses a 1D ladder-like framework constructed from CoO_3N tetrahedral, HPO_3 pseudo-pyramids and pyridine ligands. While compound **2** is an unusual inorganic–organic hybrid 1D chain, which consists of corner-shared six-membered rings made of CoO_3N_3/CoO_4N_2 octahedra and HPO_3 pseudo-pyramids through sharing vertices.

Keywords: Solvothermal synthesis; 1D chain; Cobalt (II) phosphites; Crystal structure

1. Introduction

The synthesis of transition metal phosphates with open architectures have been the focus of much scientific research owing to their interesting electrical and magnetic properties other than their conventional applications as absorbents, ion exchangers and catalysts [1–5]. Recently, the pseudo-pyramidal phosphite $[HPO_3]$ group has been investigated as a possible replacement for the traditional phosphate tetrahedron with great success [6–10]. To date, a number of studies on inorganic–organic hybrid phosphates/phosphites of various transition metals such as Fe [11–14], Cr [8,15], V [15–20], Mn [21–23] and Zn [24–32] have been carried out under hydro/solvothermal conditions. Moreover, there is also some attention to open-framework inorganic–organic hybrid cobalt phosphates and phosphites [33–41], which are obtained by the combination of the oxalate and phosphate/phosphite groups in the same crystalline material or based on organonitrogen ligands and phosphate/phosphite groups. In order to extend the knowledge about the inorganic–organic hybrid phosphites, we decide to focus our attention on the Co(II) phophites system with organic amines as ligands.

Herein, we report the syntheses, crystal structures and magnetic properties of two new inorganic–organic hybrid cobalt phosphites grafted with pyridine ligands, $Co(HPO_3)(py)$ (**1**) and $[Co(OH)(py)_3][Co(py)_2][HPO_2(OH)]_3$ (**2**). To the best of our knowledge, hybrid compounds of **1** and **2** are firstly synthesized in the cobalt phosphite–pyridine system.

2. Experimental section

2.1. Materials and methods

All chemicals used during the course of this work were of reagent grade and used as received from commercial

*Corresponding author.
E-mail address: xingy202@nenu.edu.cn (Y. Xing).

0022-4596/$ - see front matter © 2008 Elsevier Inc. All rights reserved.
doi:10.1016/j.jssc.2008.01.043

sources without further purification. The X-ray powder diffraction (XRD) data were collected on a Siemens D5005 diffractometer with Cu$K\alpha$ radiation ($\lambda = 1.5418$ Å). Elemental analyses were performed on a Perkin-Elmer 2400 element analyzer. Inductively coupled plasma (ICP) analyses were carried out on a Perkin-Elmer Optima 3300DV spectrometer. Infrared (IR) spectra were recorded within the 400–4000 cm^{-1} region on a Nicolet Impact 410 FTIR spectrometer using KBr pellets. The thermalgravimetric analyses (TGA) were performed on Perkin-Elmer TGA 7 thermogravimetric analyzer in the air with a heating rate of 20 °C min^{-1}. Magnetic susceptibility data were collected over the temperature range 300–2 K at a magnetic field of 1000 Oe on a quantum design MPMS-5 SQUID magnetometer.

2.2. Synthesis of $Co(HPO_3)(py)$, 1

$Co(HPO_3)(py)$ **1** was synthesized under mild solvothermal conditions and autogenous pressure. $CoCl_2 \cdot 6H_2O$ (0.5 mmol), H_3PO_3 (2 mmol), HF (0.4 mL) and pyridine (8 mmol) were dissolved in a volume of approximately 8 mL of a mixture of water, ethanol and DMF (1:3:4 v/v). The reaction mixture was stirred until it was homogeneous, and then sealed in a 18 mL Teflon-lined stainless steel autoclave and heated at 80 °C for 3 d, followed by slow cooling down to room temperature. The light blue pillar-like single crystals were isolated by filtration, washed with anhydrous ethanol and dried in air. The ICP and elemental analysis results of **1** were consistent with the theoretical values based on the crystal data. Found for **1**: Co, 26.59; P, 13.95; C, 27.31; H, 2.90; N, 6.45 wt%. Calcd.: Co, 27.03; P, 14.21; C, 27.55; H, 2.77; N, 6.42 wt%. The IR spectrum of 1 exhibited typical peaks corresponding to the pyridine molecules (ν_{C-H}, ν_{C-N}, ν_{C-C}, 3060–3430, 1610–1450 cm^{-1}), while the bands at 1040, 995, 636 and 573 cm^{-1} are associated with the phosphite oxoanion. A single P–H stretching band at 2390 cm^{-1} indicates the presence of a crystallographically independent phophite group in the structure.

2.3. Synthesis of $[Co(OH)(py)_3][Co(py)_2][HPO_2(OH)]_3$, 2

In a typical synthesis, a reaction mixture of $CoCl_2 \cdot 6H_2O$ (0.5 mmol), H_3PO_3 (2 mmol), HF (0.4 mL) and pyridine (8 mmol) was sealed in a 18 mL Teflon-lined steel autoclave and heated at 80 °C for 3 d, and then cooled to room temperature. The solid product, consisting of single crystals in the form of pink pillar was recovered by filtration, washed with anhydrous ethanol and dried in air. The ICP and elemental analysis results of **2** were consistent with the theoretical values based on the crystal data. Found for **2**: Co, 14.87; P, 11.91; C, 38.92; H, 4.20; N, 8.94 wt%. Calcd.: Co, 15.24; P, 12.02; C, 38.83; H, 4.17; N, 9.06 wt%. The IR spectrum of **2** showed typical peaks corresponding to the pyridine molecules and hydroxyl units (ν_{O-H}, ν_{C-H}, ν_{C-N}, ν_{C-C}, 3730–2930, 1650–1540 cm^{-1}). The bands at 1120, 1058, 1003, 673 and 570 cm^{-1} are associated with the phosphite oxoanion and the band at 2420 cm^{-1} is related to the P–H groups.

While both the two compounds have been synthesized from exactly the same reaction conditions except the reaction solvent, the resulting structures show marked differences, indicating that the solvents using in the starting materials might have significant effect on the final products. Further studies are necessary to understand the roles of solvent in yielding the different structures.

2.4. Determination of crystal structure

Crystals with dimensions $0.35 \times 0.14 \times 0.13$ mm^3 for **1** and $0.25 \times 0.15 \times 0.15$ mm^3 for **2** were selected for single-crystal XRD analyses, respectively. The intensity data were collected on a Siemens SMART CCD diffractometer using graphite-monochromatic Mo$K\alpha$ radiation ($\lambda = 0.71073$ Å). Data processing was accomplished with the SAINT processing program [42]. Both structures were solved by direct methods with the SHELXTL 97 software package [43]. All non-hydrogen atoms were refined anisotropically. Two of phosphorus atoms [P(1)] and [P(2)] in compound **2** were found to be disordered over two positions with an equal occupancy, respectively, the splitting of P atoms is not uncommon in metal phosphates/phosphites [44]. Two-third of pyridine molecules in **2** were found to be disordered. For compound **1**, the H atom of the phosphorous was located in the Fourier difference map, while all H atoms bound to C atoms were positioned geometrically and refined as riding mode. The hydrogen atoms of compound **2** were placed geometrically and refined using a riding model. Experimental details for the structural determinations of two compounds are presented in Table 1. The final atomic coordinates and selected bond distances and angles are shown clearly in Tables 2 and 4 for **1** and Tables 3 and 5 for **2**, respectively. CCDC reference number 653076 for **1** and 653077 for **2**. Copies of the data can be obtained free of charge on application to CCDC, 12 Union Road, Cambridge CB2 1EZ, UK (Fax: +44 1223 336 033; e-mail: deposit@ccdc.cam.ac.uk).

3. Results and discussion

3.1. Characterization

Fig. 1(a) and (b) shows the experimental and simulated X-ray powder diffraction patterns of compounds **1** and **2**, respectively. The XRD patterns for the bulk products are in good agreement with the patterns based on single-crystal X-ray solution, indicating the purity of the as-synthesized products. The differences in reflection intensity are probably due to preferred orientations in the powder samples (Tables 4 and 5).

Table 1
Crystal data and structure refinement for the title compounds **1** and **2**

	Compound **1**	Compound **2**
Empirical formula	C5 H6 Co N O3 P	C25 H32 Co2 N5 O10 P3
Formula weight	218.01	773.33
Temperature	293(2) K	293(2) K
Wavelength	0.71073 Å	0.71073 Å
Crystal system	Monoclinic	Orthorhombic
Space group	$P2(1)/c$	$Cmcm$
a (Å)	5.3577(7)	16.3252(18)
b (Å)	7.7503(10)	15.7005(16)
c (Å)	17.816(2)	13.0440(13)
β (deg)	94.327(2)	90
Volume (Å^3)	737.67(16)	3343.4(6)
Z	4	4
D_{calc} (mg m^{-3})	1.963	1.536
Absorption coefficient (mm^{-1})	2.493	1.194
$F(000)$	436	1584
Crystal size (mm)	$0.35 \times 0.14 \times 0.13$	$0.25 \times 0.15 \times 0.15$
θ range (deg)	2.29–28.33	1.80–28.31
Limiting indices	$-7 \leqslant h \leqslant 7$ $-10 \leqslant k \leqslant 10$ $-15 \leqslant l \leqslant 23$	$-21 \leqslant h \leqslant 20$ $-14 \leqslant k \leqslant 20$ $-17 \leqslant 1 \leqslant 17$
Reflections collected	5132	12047
Reflections unique	1828 [R(int) = 0.0293]	2241 [R(int) = 0.0814]
Refinement method	Full-matrix least-squares on F^2	Full-matrix least-squares on F^2
Data/restraints/parameters	1828/0/92	2241/0/170
Goodness-of-fit on F^2	1.068	1.036
Final R indices [$I > 2\sigma(I)$]	$R_1 = 0.0424$, w$R_2 = 0.1162$	$R_1 = 0.0442$, w$R_2 = 0.1205$
R indices (all data)	$R_1 = 0.0541$, w$R_2 = 0.1274$	$R_1 = 0.0794$, w$R_2 = 0.1376$
Largest diff. peak and hole (e Å^{-3})	0.939 and −1.024	0.486 and −0.485

Table 2
Atomic coordinates ($\times 10^4$) and equivalent isotropic displacement parameters (Å$^2 \times 10^3$) for **1**

	x	y	z	U (eq)
Co(1)	1931(1)	1016(1)	4173(1)	23(1)
P(1)	−2919(2)	2403(1)	4877(1)	30(1)
O(1)	−1489(6)	1750(6)	4238(2)	49(1)
O(2)	2423(7)	−1382(4)	4405(2)	47(1)
O(3)	4334(6)	2605(4)	4634(2)	43(1)
N(1)	2261(5)	1160(4)	3038(1)	33(1)
C(1)	4254(4)	2010(4)	2746(1)	38(1)
C(2)	4386(5)	2121(4)	1971(1)	45(1)
C(3)	2524(6)	1381(5)	1489(1)	43(1)
C(4)	531(5)	530(5)	1782(1)	47(1)
C(5)	399(4)	419(4)	2557(2)	42(1)

Table 3
Atomic coordinates ($\times 10^4$) and equivalent isotropic displacement parameters (Å$^2 \times 10^3$) for **2**

	x	y	z	U (eq)
Co(1)	5000	2788(1)	2500	30(1)
Co(2)	5000	0	0	31(1)
P(1)	4761(1)	2178(1)	116(1)	33(1)
P(2)	5281(1)	−647(1)	2500	31(1)
O(1)	5000	1444(3)	2500	61(2)
O(2)	5000	2825(2)	919(2)	38(1)
O(3)	5000	1294(2)	352(2)	50(1)
O(4)	5000	2483(2)	−920(3)	87(2)
O(5)	5000	−217(2)	1543(2)	45(1)
O(6)	5000	−1596(3)	2500	55(1)
N(1)	5000	4172(3)	2500	35(1)
N(2)	3667(3)	2737(2)	2500	46(1)
N(3)	3652(3)	0	0	46(1)
C(1)	5000	4623(3)	1640(4)	71(2)
C(2)	5000	5508(3)	1611(4)	74(2)
C(3)	5000	5949(4)	2500	50(2)
C(4)	3280(6)	2212(6)	1830(7)	76(3)
C(4′)	3221(5)	3187(5)	1874(6)	57(2)
C(5)	2417(7)	2140(8)	1852(10)	108(4)
C(5′)	2357(5)	3148(6)	1850(8)	75(3)
C(6)	1966(5)	2617(6)	2500	85(2)
C(7)	3251(6)	−594(7)	483(9)	91(3)
C(7′)	3210(5)	393(6)	741(6)	61(2)
C(8)	2401(8)	−625(10)	484(11)	120(5)
C(8′)	2351(7)	417(7)	754(9)	84(3)
C(9)	1936(5)	0	0	96(3)

Table 4
Selected bond lengths (Å) and bond angles (deg) for **1**

Co(1)–O(2)	1.918(4)	P(1)–O(1)	1.507(3)
Co(1)–O(3)	1.921(3)	P(1)–O(2)#1	1.510(4)
Co(1)–O(1)	1.930(3)	P(1)–O(3)#2	1.511(3)
Co(1)–N(1)	2.0460(19)	P(1)–H(1)	1.38(4)
O(2)–Co(1)–O(3)	116.92(15)	O(1)–P(1)–O(2)#1	113.4(2)
O(2)–Co(1)–O(1)	112.85(17)	O(1)–P(1)–O(3)#2	110.97(19)
O(3)–Co(1)–O(1)	113.22(15)	O(2)#1–P(1)–O(3)#2	113.7(2)
O(2)–Co(1)–N(1)	104.17(13)	O(1)–P(1)–H(1)	106.4(18)
O(3)–Co(1)–N(1)	106.40(13)	O(2)#1–P(1)–H(1)	102.3(18)
O(1)–Co(1)–N(1)	101.30(12)	O(3)#2–P(1)–H(1)	109.4(17)

Symmetry transformations used to generate equivalent atoms: #1 $-x$, $-y$, $-z+1$, #2 $x-1$, y, z.

In order to examine the thermal stability of **1** and **2**, TGA under air atmosphere were carried out. The TGA diagrams for **1** and **2** are given in Fig. 2. TG analysis for **1** shows a total weight loss of 32.60 wt% in the region 60–550 °C, which is attributed to the loss of pyridine molecules (calcd. 33.07 wt%). The TG curve of compound **2** exhibited a total weight loss of 59.10 wt% around 60–800 °C, corresponding to the loss of five organic amine molecules (calcd. 51.14 wt%) and four hydroxyl units (Calcd. 8.80 wt%). XRD analyses indicated that the title compound **1** became $Co_2P_2O_7$, and compound **2** appeared to be an unidentified phase after the decomposition of the occluded template molecules.

Table 5
Selected bond lengths (Å) and bond angles (deg) for **2**

Co(1)–O(2)	2.064(3)	Co(2)–N(3)	2.201(4)
Co(1)–O(2)#1	2.064(3)	P(1)–O(3)	1.475(3)
Co(1)–O(1)	2.109(4)	P(1)–O(4)	1.486(3)
Co(1)–N(1)	2.174(5)	P(1)–O(2)	1.510(3)
Co(1)–N(2)	2.177(4)	P(2)–O(5)#1	1.492(3)
Co(1)–N(2)#2	2.177(4)	P(2)–O(5)	1.492(3)
Co(2)–O(5)	2.041(3)	P(2)–O(6)	1.559(5)
Co(2)–O(3)	2.082(3)		
O(2)–Co(1)–O(2)#1	176.72(15)	O(5)#3–Co(2)–O(3)	93.16(12)
O(2)–Co(1)–O(1)	91.64(8)	O(5)–Co(2)–O(3)	86.84(12)
O(2)–Co(1)–N(1)	88.36(8)	O(3)–Co(2)–O(3)#3	180.00(3)
O(1)–Co(1)–N(1)	180.0	O(5)–Co(2)–N(3)	90.0
O(2)–Co(1)–N(2)	90.060(4)	O(3)–Co(2)–N(3)	90.0
O(1)–Co(1)–N(2)	87.92(10)	N(3)–Co(2)–N(3)#3	180.0
N(1)–Co(1)–N(2)	92.08(10)	O(3)–P(1)–O(4)	115.02(19)
O(2)–Co(1)–N(2)#2	90.060(4)	O(3)–P(1)–O(2)	114.86(17)
O(1)–Co(1)–N(2)#2	87.92(10)	O(4)–P(1)–O(2)	110.26(18)
N(1)–Co(1)–N(2)#2	92.08(10)	O(5)#1–P(2)–O(5)	113.7(2)
N(2)–Co(1)–N(2)#2	175.8(2)	O(5)–P(2)–O(6)	110.01(13)
O(5)#3–Co(2)–O(5)	180.00(16)		

Symmetry transformations used to generate equivalent atoms: #1 x, y, $-z+1/2$, #2 $-x+1$, y, $-z+1/2$, #3 $-x+1$, $-y$, $-z$.

3.2. Structure determination of **1** and **2**

As shown in Fig. 3(a), the asymmetric unit of compound **1** contains 11 independent non-hydrogen atoms, including one cobalt (II) atom, one phosphorus atom, three oxygen atoms, five carbon atoms and one nitrogen atom. The cobalt atom is coordinated by three oxygen atoms from phosphite anions and one nitrogen atom of the pyridine molecule to form a CoO_3N tetrahedron, which is consistent with the blue color of compound **1**. The average Co–O bond length is 1.923(3) Å and Co–N bond length is 2.0460(19) Å, whereas the coordination angles around Co atom are in the range of 101.30(12)–116.92(15)°. The phosphorus atom bonds to three oxygen atoms with adjacent Co atom with P–O bond lengths ranging from 1.507(3) to 1.511(3) Å, and to a proton with P–H = 1.38(4) Å, completing a pseudo-pyramid coordination characteristic of phosphorus (III). The O–P–H and O–P–O bond angles are in the range of 102.3(18)–113.7(2)°.

The structure of **1** consists of a network of tetrahedral CoO_3N and pseudo-tetrahedral HPO_3 units, strictly alternating, connected through their vertices to give rise to a 4-membered ring (Co_2P_2, not counting four bridging oxygen sites). The 4-membered rings are further linked through their edges forming neutral one-dimensional (1D) ladder-like chains, which propagate along the *a*-axis. (Fig. 3b). These 4-ring chains adopt a double "zigzag" geometry, akin to the partial tetrahedral connectivity in three-dimensional aluminosilicate zeolites such as the ABW network [45]. The pyridine ligands are attached to the cobalt atoms and extend to each side of the ladder structure. This arrangement is similar in profile to the ladder-like chains of zinc phosphates [24,46], zinc phosphites [47] and zinc sulfite [48]. The 3D structure packing diagram of **1** is shown in Fig. S1(a) (supporting information). The neutral chains in **1** are held together by van der Waals forces.

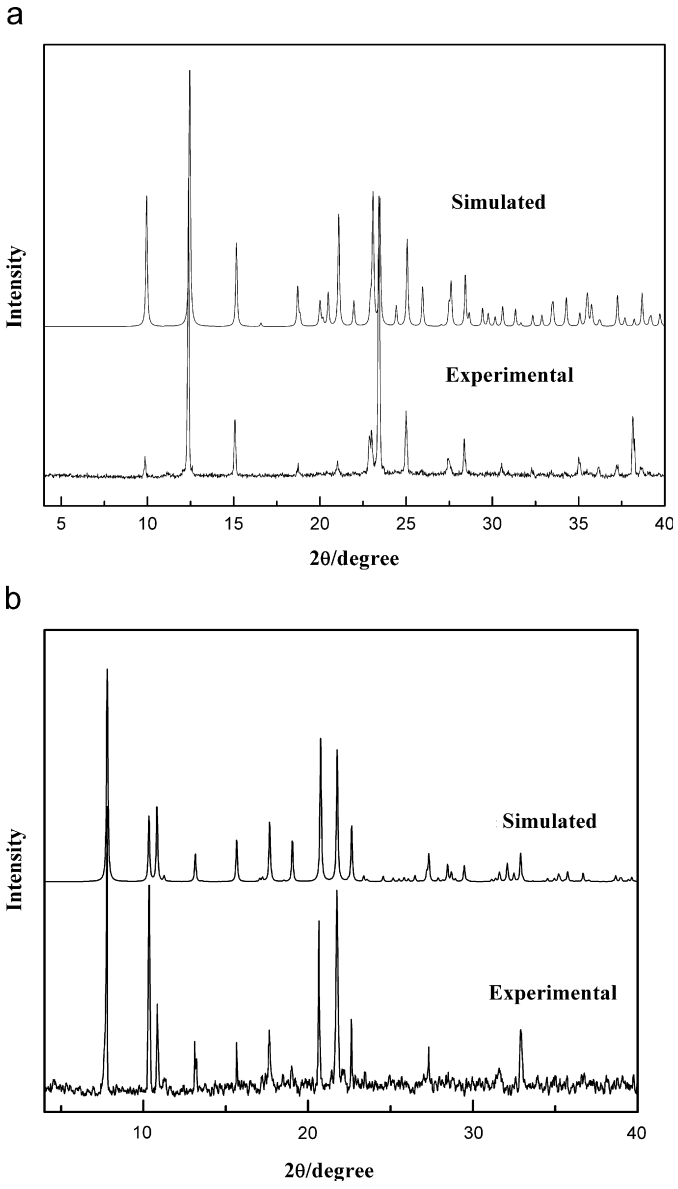

Fig. 1. Simulated and experimental powder X-ray diffraction patterns of **1** (a) and **2** (b).

The asymmetric unit of **2**, as seen in Fig. 4(a), contains two crystallographically distinct Co atoms. The Co(1) atom is coordinated by three nitrogen atoms from three pyridine and two oxygen atoms from two phosphite anions, the remaining connection needed for the octahedral linkage with Co(1) comes from a terminal bond having a oxygen atom of hydroxyl unit (Co(1)–O(1)~2.109(4) Å). The coordination angles around the Co(1) ion are in the range of 87.92(10)–180.0°, to give a slightly distorted octahedral coordination geometry. The Co(2) atom is octahedrally coordinated by two nitrogen atoms from two

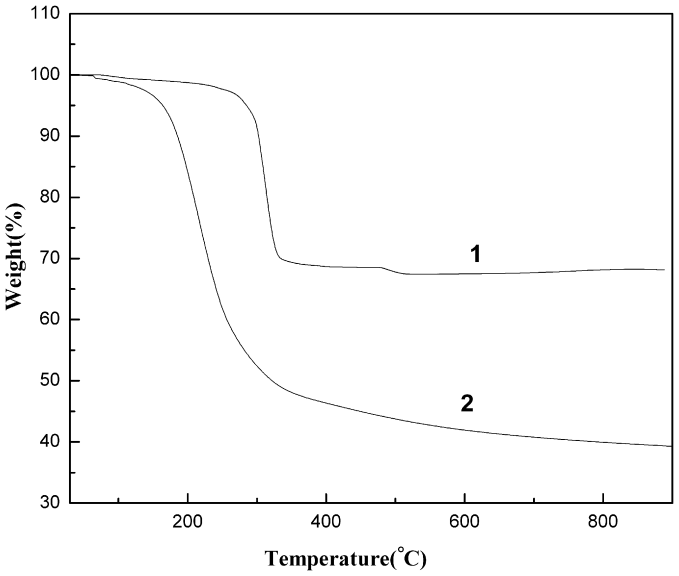

Fig. 2. The TG curves of **1** and **2** under air atmosphere.

pyridine and four oxygen atoms from four phosphite anions to give a slightly distorted octahedral geometry with coordination angles in the range of 86.84(12)–180.0°. Of the two crystallographically distinct P atoms, P(1) and P(2) each share two oxygen atoms with adjacent Co atoms [P–O: 1.475(3)–1.510(3) Å] and possess one terminal P–OH bonds [P–O: 1.486(3) Å for **1** and 1.559(5) Å for **2**], with the fourth ligand being a terminal P–H bond. These values are within the expected ranges.

The building block of the framework of **2** contains three CoO_3N_3/CoO_4N_2 octahedra and three HPO_3 pesudo-pyramids, which are linked alternatively by sharing vertices and form a six-membered ring. The six-membered rings are further linked through vertex Co(2) atom resulting in neutral inorganic–organic hybrid 1D chains, which propagate along the *c*-axis. (Fig. 4(b)). One of the most striking aspects of **2** is the presence of the corner-shared six-membered rings chains, which is very unusual in metal phosphates/phosphites. The 3D structure packing diagram of **2** is shown in Fig. S1(b) (supporting information).

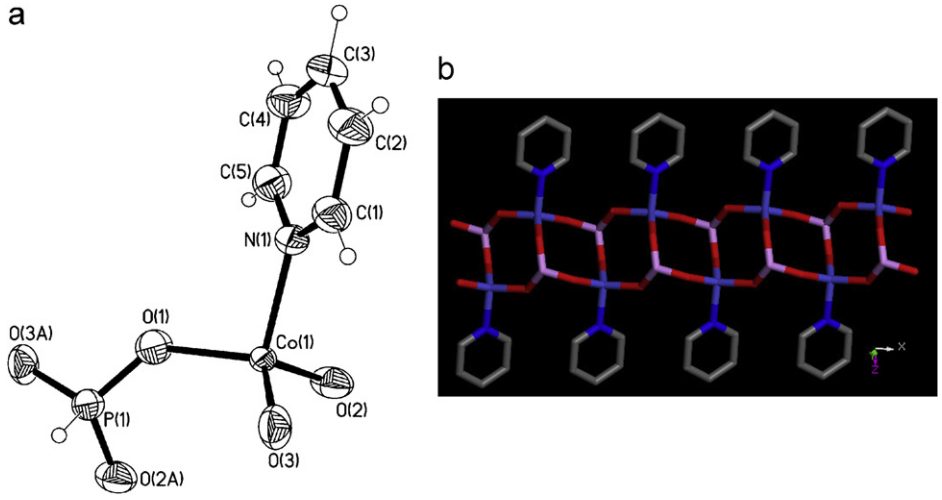

Fig. 3. (a) ORTEP diagram of **1** showing the local coordination environment and connectivity between inorganic and organic components. (b) The ladder structure with bonded pyridine molecules extending to each side of the ladder. Light blue, Co; Pink, P; Red, O; Blue, N.

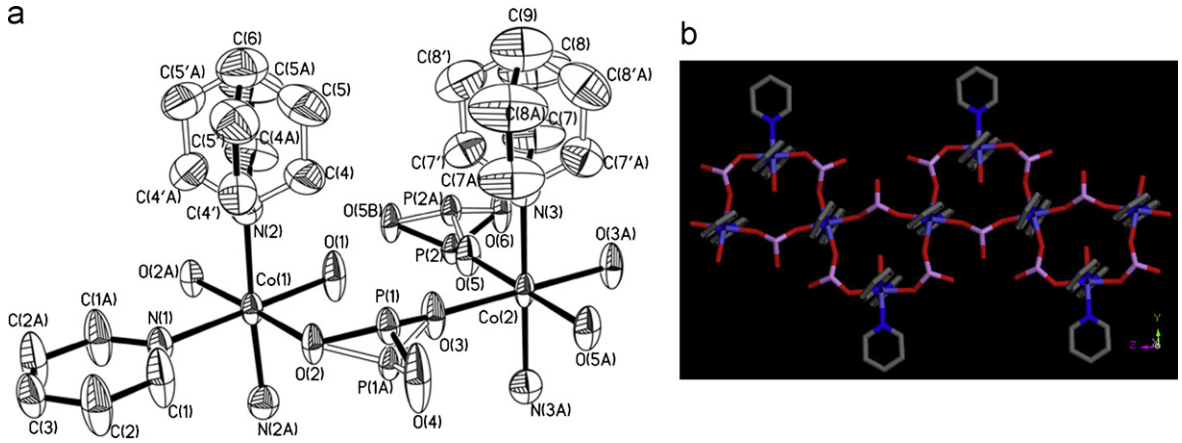

Fig. 4. (a) ORTEP diagram of **2** showing the local coordination environment and connectivity between inorganic and organic components. (b) 1D chain consists of corner-shared six-membered rings propagate along the *c*-axis.

3.3. Magnetic properties

Variable temperature magnetic susceptibility measurements have been performed on powdered samples in the range from 2.0 to 300 K. Fig. S2(a) and (b) (supporting information) show the plots of the χ_m and $\chi_m T$ vs. T curves of compounds **1** and **2**, respectively. The results show that compound 1 is diamagnetic. While for compound **2**, the molar magnetic susceptibility increase with decreasing temperature in all the temperature range studied and follows the Curie–Weiss law at temperature above 50 K with $C = 4.239\,cm^3\,K\,mol^{-1}$ and $\theta = -18.35\,K$. The $\chi_m T$ vs. T curve continuously decreases from $3.99\,cm^3\,K\,mol^{-1}$ at 300 K to $2.55\,cm^3\,K\,mol^{-1}$ at 2.0 K. These results indicate the existence of antiferromagnetic interactions in compound **2**.

4. Conclusions

Two novel inorganic–organic hybrid 1D cobalt (II) phosphites $Co(HPO_3)$ (py) (**1**) and $[Co(OH)(py)_3][Co(py)_2][HPO_2(OH)]_3$ (**2**), were obtained as good-quality single crystals under solvothermal conditions in the presence of pyridine. Structural analyses indicate that compound **1** is a 1D ladder structure constructed by edge-shared four-membered rings. Compound **2** is an unusual inorganic–organic hybrid 1D chains, which consist of corner-shared six-membered rings made of CoO_3N_3/CoO_4N_2 octahedra and HPO_3 pseudo-pyramids through sharing vertices. Both of the compounds possess neutral frameworks with the organic amines bonded directly to the cobalt centers. Studies on more new inorganic–organic hybrid materials in this field are in progress.

Acknowledgments

This work was supported by Training Fund of NENU'S Scientific Innovation Project (no. NENU-STC07004) and the Analysis and Testing Foundation of Northeast Normal University.

Appendix A. Supporting Information

Supplementary data associated with this article can be found in the online version at doi:10.1016/j.jssc.2008.01.043.

References

[1] A.K. Cheetham, G. Férey, T. Loiseau, Angew. Chem. Int. Ed. 38 (1999) 3268.
[2] Y.C. Jiang, S.L. Wang, K.H. Lii, Chem. Mater. 15 (2003) 1633.
[3] A. Choudhury, S. Neeraj, S. Natarajan, C.N.R. Rao, Angew. Chem. Int. Ed. 39 (2000) 3091.
[4] C.N.R. Rao, S. Natarajan, S. Neeraj, J. Am. Chem. Soc. 122 (2000) 2810.
[5] A.M. Chippindale, F.O.M. Gaslain, A.R. Cowley, A.V. Powell, J. Mater. Chem. 11 (2001) 3172.
[6] J.A. Rodgers, W.T.A. Harrison, Chem. Commun. (2000) 2385.
[7] J. Liang, J.Y. Li, J.H. Yu, P. Chen, Q.R. Fang, F.X. Sun, R.R. Xu, Angew. Chem. Int. Ed. 45 (2006) 2546.
[8] S. Fernández, J.L. Mesa, J.L. Pizarro, L. Lezama, M.I. Arriortua, T. Rojo, Angew. Chem. Int. Ed. 41 (2002) 3683.
[9] U.-C. Chung, J.L. Mesa, J.L. Pizarro, L. Lezama, J.S. Garitaonandia, J.P. Chapman, M.I. Arriortua, J. Solid State Chem. 177 (2004) 2705.
[10] Y.L. Yang, N. Li, H.B. Song, H.G. Wang, W.B. Chen, S.H. Xiang, Chem. Mater. 19 (2007) 1889.
[11] W.J. Chang, Y.C. Jiang, S.L. Wang, K.H. Lii, J. Solid State Chem. 179 (2006) 3059.
[12] N. Rajic, D. Stojakovic, D. Hanzel, N.Z. Logar, V. Kaucic, Micropor. Mesopor. Mater. 55 (2002) 313.
[13] S. Mandal, S.K. Pati, M.A. Green, S. Natarajan, Chem. Mater. 17 (2005) 638.
[14] S. Fernandez, J.L. Mesa, J.L. Pizarro, J.S. Garitaonaindia, M.I. Arriotua, T. Rojo, Angew. Chem. Int. Ed. 43 (2004) 977.
[15] S. Fernandez, J.L. Mesa, J.L. Pizarro, L. Lezama, M.I. Arriortual, T. Rojo, Chem. Mater. 15 (2003) 1204.
[16] C.H. Huang, L.H. Huang, K.H. Lii, Inorg. Chem. 40 (2001) 2625.
[17] J. Do, R.P. Bontchev, A.J. Jacobson, Inorg. Chem. 39 (2000) 3230.
[18] M. Tang, K. Lii, J. Solid State Chem. 177 (2004) 1912.
[19] G. Bonavia, J. DeBord, R.C. Haushalter, D. Rose, J. Zubieta, Chem. Mater. 7 (1995) 1995.
[20] S. Fernandez, J.L. Mesa, J.L. Pizarro, L. Lezama, M.I. Arriortua, T. Rojo, Chem. Mater. 14 (2002) 2300.
[21] R. Yu, X. Xing, T. Saito, M. Azuma, M. Takano, D. Wang, Y. Chen, N. Kumada, N. Kinomura, Solid State Sci. 7 (2005) 221.
[22] S. Fernandez, J.L. Mesa, J.L. Pizarro, L. Lezama, M.I. Arriortua, R. Olazcuaga, T. Rojo, Chem. Mater. 12 (2000) 2092.
[23] S. Fernandez, J.L. Mesa, J.L. Pizarro, L. Lezama, M.I. Arriortua, R. Olazcuaga, T. Rojo, Inorg. Chem. 40 (2001) 3476.
[24] J. Fan, C. Slebodnick, R. Angel, B.E. Hanson, Inorg. Chem. 44 (2005) 552.
[25] L. Wang, M. Yang, G.H. Li, Z. Shi, S.H. Feng, J. Solid State Chem. 179 (2006) 156.
[26] W.T.A. Harrison, R.M. Yeates, M.L.F. Phillips, T.M. Nenoff, Inorg. Chem. 42 (2003) 1493.
[27] Z.E. Lin, J. Zhang, S.T. Zheng, Q.H. Wei, G.Y. Yang, Solid State Sci. 5 (2003) 1435.
[28] J. Liang, Y. Wang, J.H. Yu, Y. Li, R.R. Xu, Chem. Commun. (2003) 882.
[29] W.T.A. Harrison, M.L.F. Phillips, J. Stanchfield, T.M. Nenoff, Inorg. Chem. 40 (2001) 895.
[30] J.X. Pan, S.T. Zheng, G.Y. Yang, Micropor. Mesopor. Mater. 75 (2004) 129.
[31] Z.E. Lin, J. Zhang, S.T. Zheng, G.Y. Yang, Micropor. Mesopor. Mater. 68 (2004) 65.
[32] Z.E. Lin, W. Fan, F.F. Gao, N. Chino, T. Yokoi, T. Okubo, Cryst. Growth Des. 6 (2006) 2435.
[33] W.K. Chang, R.K. Chiang, Y.C. Jiang, S.L. Wang, S.F. Lee, K.H. Lii, Inorg. Chem. 43 (2004) 2564.
[34] T. Huang, B.A. Vanchura, Y.K. Shan, S.D. Huang, J. Solid State Chem. 180 (2007) 2110.
[35] A. Choudhury, S. Natarajan, Solid State Sci. 2 (2000) 365.
[36] S. Ekambaram, S.C. Sevov, J. Mater. Chem. 10 (2000) 2522.
[37] W.K. Chang, R.K. Chiang, S.L. Wang, J. Solid State Chem. 180 (2007) 1713.
[38] S. Fernandez, J.L. Pizarro, J.L. Mesa, L. Lezama, M.I. Arriortua, T. Rojo, Int. J. Inorg. Mater. 3 (2001) 331.
[39] S. Mandal, S. Natarajan, J. Solid State Chem. 178 (2005) 2376.
[40] J. Fan, G.T. Yee, G. Wang, B.E. Hanson, Inorg. Chem. 45 (2006) 599.
[41] J.H. Liao, P.L. Chen, C.C. Hsu, J. Phys. Chem. Solids 62 (2001) 1629.
[42] SMART and SAINT (Software Package), Siemens Analytical X-ray Instruments Inc., Madison, WI, 1996.

[43] G. M. Sheldrick, SHELXL Program, Version 5.1, Siemens Industrial Automation, Inc., Madison, WI, 1997.
[44] (a) V. Zima, K.H. Lii, Chem. Mater. 10 (1998) 1914;
(b) Z. Shi, D. Zhang, G.H. Li, L. Wang, X.Y. Lu, J. Hua, S.H. Feng, J. Solid State Chem. 172 (2003) 464.
[45] J.V. Smith, Chem. Rev. 88 (1988) 149.
[46] A.A. Ayi, A. Choudhury, S. Natarajan, S. Neeraj, C.N.R. Rao, J. Mater. Chem. 11 (2001) 1181.
[47] J. Fan, C. Slebodnick, D. Troya, R. Angel, B.E. Hanson, Inorg. Chem. 44 (2005) 2719.
[48] C. Austria, J. Zhang, H. Valle, Q. Zhang, E. Chew, D.T. Nguyen, J.Y. Gu, P.Y. Feng, X.H. Bu, Inorg. Chem. 46 (2007) 6283.